

# Hydrogen Aging During Hole Expanding Tests of Galvanized High Strength Steels Investigated Using a Novel Thermal Desorption Analyzer for Small Samples

Mélie Mandy<sup>1,†</sup>, Maïwenn Larnicol<sup>1</sup>, Louis Bordignon<sup>1</sup>, Anis Auaf<sup>2</sup>,  
Mihaela Teaca<sup>2</sup>, and Thierry Sturel<sup>2</sup>

<sup>1</sup>CRM Group, Liège, Belgium

<sup>2</sup>ArcelorMittal Global R&D, Maizières-lès-Metz, France

(Received January 17, 2024; Revised January 17, 2024; Accepted March 25, 2024)

In the automotive industry, the hole expanding test is widely used to assess the formability of punched holes in sheets. This test provides a good representation of formability within the framework defined by the ISO 16630 standard. During hole expanding tests on galvanized high strength steels, a negative effect was observed when there was a delay between hole punching and expansion, as compared to performing both operations directly. This effect is believed to be caused by hydrogen aging, which occurs when hydrogen diffuses towards highly-work hardened edges. Therefore, the aim of this study is to demonstrate the migration of hydrogen towards work-hardened edges in high strength Zn-coated steel sheets using a novel Thermal Desorption Analyzer (TDA) designed for small samples. This newly-developed TDA setup allows for the quantification of local diffusible hydrogen near cut edges. With its induction heating and ability to analyze Zn-coated samples while reducing artifacts, this setup offers flexible heat cycles. Through this method, a hydrogen gradient is observed over short distances in shear-cut galvanized steel sheets after a certain period of time following punching.

**Keywords:** Hydrogen aging, Automotive industry, Hole expanding test, Thermal desorption

## 1. Introduction

Advanced high strength steels constitute a key material for tackling the challenges of the automotive industry. Among them, dual-phase (DP) steels exhibit very interesting mechanical properties such as a combination of high tensile strength and elongation. They continue to offer a key asset for current challenges of the automotive industry, aiming at guaranteeing safety (through the use of resistant materials) while continuing to reduce vehicle weight for economic and ecologic reasons [1].

In the automotive industry, a wide range of processes are implemented to transform steel sheets into car body-in-whites : shearing, bending, stamping, ... Among them, a critical process consists in bending cut or punched edges, which can induce an embrittlement of advanced high strength steels. In this context, the ISO 16630 standard [2] aims at assessing the ability of a given material to be formed, through a hole punching and expanding sequence. A hole is first punched according to specific dimensions

and clearances in the tested steel sheet. This hole is then expanded by the application of a cone at a given rate until a first crack appears around the hole, which indicates the end of the test. The result of this test is expressed as a hole diameter increase ratio, based on the reproduction of several trials [2].

In this standard, no specific indication is given about the time between punching and expanding the hole. In practice, long time can be expected between those operations, as they require the use of different tools. Previous works have shown that this time between hole punching and expansion could in some circumstances impact the hole expansion capability [3,4]. This phenomenon was observed on galvanized DP steels: a detrimental effect occurs when a longer time is applied compared to direct succession of both operations. This effect is assumed to be related to hydrogen aging enabled by the diffusion of hydrogen present in the metal towards highly work-hardened edges.

In this context, this work aims at evidencing hydrogen migration towards work-hardened edges in high strength

<sup>†</sup>Corresponding author: [melodie.mandy@crmgroup.be](mailto:melodie.mandy@crmgroup.be)

Zn-coated steel sheets and more specifically in DP780GI steel grades. Work-hardened edges are in this case generated by shear-cutting, rather than by punching, for logistic reasons. The specific methodology developed to study this topic will be presented in the next section and consists in comparing diffusible hydrogen contents in metallic sheets either straightforwardly after shearing or after several hours after shearing. This study was enabled by the use of a newly developed TDA set-up dedicated to small samples ensuring to quantify diffusible hydrogen near cut edges. Based on induction heating, this set-up indeed offers very flexible heat cycles, the ability to analyze samples without Zn removal and a reduction of measurement artifacts.

## 2. Experimental Method

### 2.1 Material and sample preparation

For this study, material is constituted of a 2 mm-thick galvanized dual-phase steel, exhibiting a strength of about 780 MPa. More specifically, two different DP780GI were analyzed. This material exhibits a ferrite – martensite microstructure and a zinc coating applied through hot-dip galvanization on both faces. For the purpose of this study, the two DP780 steel grades were produced using different annealing conditions (before galvanizing): one of the two DP780 was subjected to specific annealing conditions in order to obtain a very high initial hydrogen content.

In order to study hydrogen migration towards cut edges, the following strategy was followed. 200-by-300 mm steel sheets were cut into two similar pieces through shear-cutting. One piece was directly stored in liquid nitrogen, in order to freeze hydrogen diffusion within it, while the other piece was aged during 48 h at room temperature and ambient pressure. After this time delay, 3 mm-wide strips were cut on both pieces, starting from the initial shear-cut edge and going to the bulk. Their position with respect to the initial shear cut was clearly noted. On each 3 mm-wide strip, 10 mm-long samples were collected to be analyzed using Thermal Desorption Analysis (TDA). Except for the 48 h-aging of the large piece at room temperature, samples were always stored in liquid nitrogen between each cutting / preparation operation and time spent at room temperature is minimized to the strict necessity of operations.

Some samples underwent specific operations before thermal desorption analysis. They were pickled, in order to remove zinc coating. This was performed using the immersion in a solution constituted of HCl in H<sub>2</sub>O, to which 3.5 g/L of HMTA inhibitor was added. Samples were immersed in the pickling solution. When bubbling stopped, the Zn coating was considered to be fully dissolved. The samples were then removed from the solution and rinsed using distilled water before being dried and stored in liquid nitrogen or directly analyzed using TDA.

Some other samples were not pickled but exposed to a degassing heat treatment, which consisted in a heat treatment of 180 °C during 1h in a furnace, without control of the atmosphere.

### 2.2 Thermal desorption analysis (TDA)

Diffusible hydrogen content of the samples was determined using Thermal Desorption Analysis. The principle is the following (Fig. 1): samples are placed in an isolated chamber where they are heated at a given heating rate so that their absorbed hydrogen content can desorb, recombine and be carried away by an inert carrier gas until mass spectrometer.

For the sake of this study, a home-made set-up was developed at CRM Group in order to analyze small samples (Fig. 1 and 2). This equipment is based on

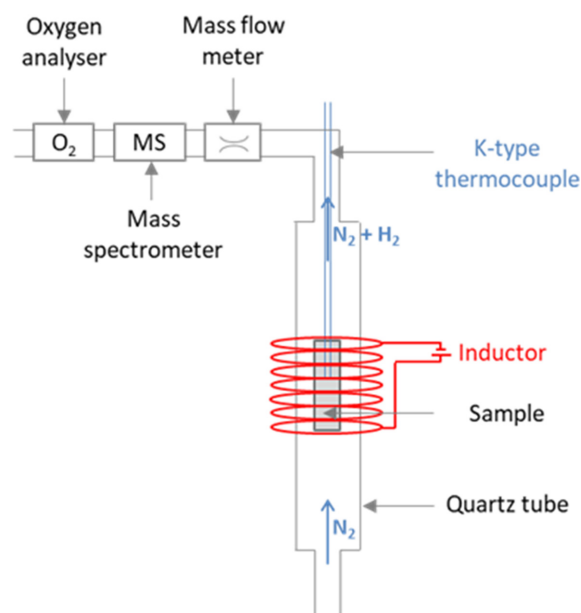


Fig. 1. Principle of Thermal Desorption Analysis

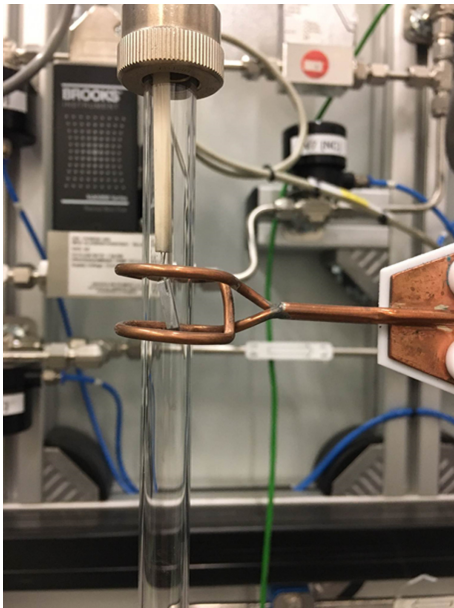


Fig. 2. Picture of newly-developed TDA set-up for small samples at CRM Group

induction heating, offering a very good flexibility in terms of heat treatment and a good heating homogeneity for such small samples. It is also based on smaller dimensions of tubes and chambers, in order to analyze samples down to 1g. The samples dimensions must fit within a quartz cylinder of 12 mm-large internal diameter. This feature enables to obtain very local information of the diffusible hydrogen content within a larger component. Furthermore, as samples are smaller, diffusion through the bare edges is enhanced and ensures to analyze diffusible hydrogen content, without removing a hydrogen barrier coating, as zinc for instance. Finally, some improvements in terms of noise and external contamination were noticed, due to a very localized heating enabled by induction heating.

In this study, except for some specific conditions which will be clearly indicated, samples were always analyzed with their GI coating (no zinc removal was performed before TDA). 3-by-10 mm coupons were heated at a rate of 20 °C/min until 400 °C, except for specific conditions where heating rate was varied between 5 and 40 °C/min. The diffusible hydrogen content was obtained by integrating hydrogen desorption spectrum until the end of the peak. The result is expressed in terms of wt. ppm of hydrogen in the steel sample. In all cases, the result is the mean value of at least 3 different tests and the error bars refer to the standard deviation with respect to this mean value.

### 2.3 Kissinger's methodology for hydrogen de-trapping energy determination

Kissinger's methodology enables the determination of the activation energy for hydrogen desorption from different traps in the metal. An activation energy can be computed from each hydrogen desorption peak contribution. The desorption activation energy is calculated based on Kissinger's work [5] and on the method explained by Bergers *et al.* [6] from equation (1):

$$\frac{\partial \ln\left(\frac{\Phi}{T_p^2}\right)}{\partial\left(\frac{1}{T_p}\right)} = -\frac{E_A}{R} \quad (1)$$

where:

- $\Phi$  is the desorption heating rate (in K/min);
- $T_p$  corresponds to the temperature of the maximum of the hydrogen desorption spectrum (in K);
- $E_A$  is the activation energy for hydrogen de-trapping (in kJ/mol);
- $R$  is the ideal gas constant, this is, 8.314 J/mol<sup>-1</sup>K<sup>-1</sup>.

### 3. Results

Firstly, the diffusible hydrogen content was measured in a reference sample, collected in the bulk of the steel sheets, and is exhibited for both studied DP780GI steel grades in Table 1. As observed, reference diffusible content present in steel grade 1 is far larger than in steel grade 2 (almost 10 times larger).

Fig. 3 shows the profiles of diffusible hydrogen contents measured in both steel grades, either after direct measurement (in blue) or after 48 h-aging in ambient conditions (in red). The green dashed line represents the reference bulk content, as displayed in Table 1. The distance from the cut edge is reported on the x-axis and is defined as the center of the collected samples. For example, samples from the 1<sup>st</sup> 3 mm-large strip next to

Table 1. Diffusible hydrogen contents measured in the bulk of both studied DP780GI steel grades

	Reference diffusible hydrogen content [wt.ppm]
Steel grade 1	0.55 ± 0.03 ppm
Steel grade 2	0.06 ± 0.04 ppm

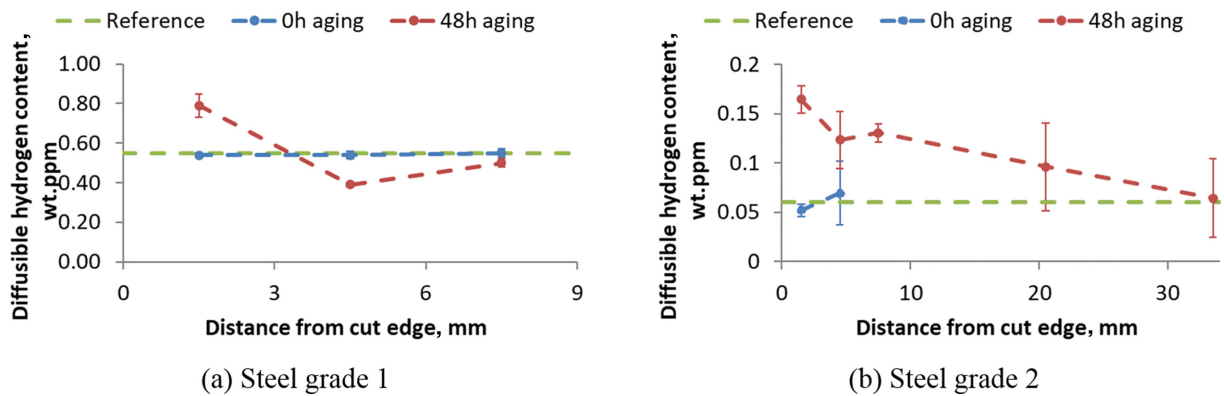


Fig. 3. Diffusible hydrogen content profiles starting from the cut edge to the bulk material for (a) steel grade 1 and (b) steel grade 2. As observed, the y-axis scale of both graphs is quite different, for a better observation of trends

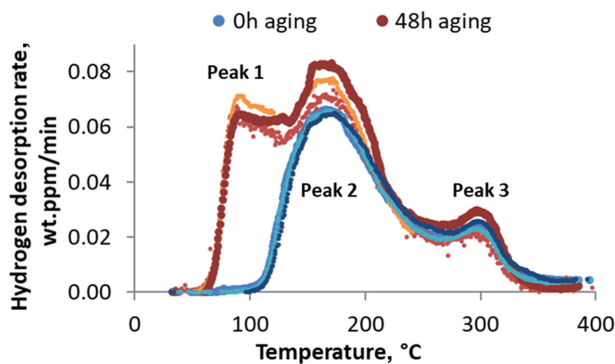


Fig. 4. Hydrogen desorption spectra obtained for samples originating from the 1<sup>st</sup> 3mm-layer near the cut edge of steel grade 1, either on the 48 h-aged (reddish curves) or on the 0h-aged steel sheet (bluish curves)

the cut edge are positioned by their center at 1.5 mm, and so on... As observed, direct measurements highlight a good homogeneity of diffusible hydrogen contents in that steel piece. However, a segregation near the cut edge is observed when the steel piece is aged during 48 h. The distance on which this hydrogen gradient exists is also very different for each steel grade.

As steel grade 1 offers exacerbation of diffusible hydrogen differences, through its larger reference content, next investigations were focused on it. A selection of hydrogen desorption spectra associated with Fig. 3a results for steel grade 1 is illustrated in Fig. 4. More specifically, those results correspond only to samples originating from the 1<sup>st</sup> 3 mm-large strip collected near the shear-cut edge, either for the steel sheet that was not aged (bluish curves) or for the 48h-aged steel piece (reddish curves). This selection was made in order to illustrate the good reproducibility of TDA measurements for 3 samples

per condition. It was not enlarged to the other strips because all the other hydrogen desorption spectra (aged or not) actually superposed with bluish curves (0 h aging) and thus did not bring further information. Those spectra express the hydrogen desorption rate as a function of desorption temperature during TDA experiments. Fig. 4 highlights also the fact that two contributions to the desorption peak are observed for samples collected on the steel sheet that was not exposed to aging (bluish curves, peaks 2 and 3). For the steel sheet exposed to 48h-aging (reddish curves), a third contribution (additional peak 1) appears at very low desorption temperature.

In order to better understand the origin of the two or three contributions to the desorption peaks, different heating rates were applied on samples collected on the 1<sup>st</sup> 3 mm-large strip of both pieces of steel grade 1. The heating rate was varied between 5 and 40 °C/min. Some hydrogen desorption spectra are illustrated in Fig. 5, in order to observe the slight shift of the peaks. Indeed, as the heating rate decreases, the peaks tend to shift to slightly lower desorption temperatures. Furthermore, as the graph is represented as a function of temperature, the desorption spectra also seem to be smaller in intensity. However, the total diffusible content is well conserved for all samples, as the time effect is not visible on this graph (different heating rates imply different desorption durations for the studied samples).

Based on Fig. 5 analysis, Kissinger's methodology was applied to obtain de-trapping energies for hydrogen during desorption. The latter are summarized in Table 2, still focused on steel grade 1.

Fig. 6 and Fig. 7 highlight the effects of degassing and

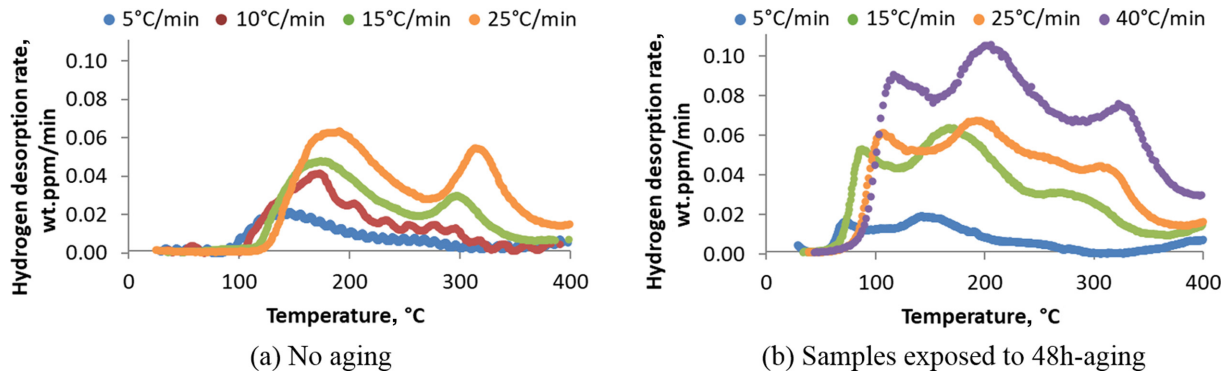


**Fig. 5. Hydrogen desorption spectra obtained for samples originating from the 1<sup>st</sup> 3 mm-layer near the cut edge of steel grade 1 using various heating rates in TDA. Samples were either collected (a) on the steel sheet that was not aged or (b) on the steel sheet that was aged during 48 h in ambient conditions**

**Table 2. Activation energies for hydrogen de-trapping in steel grade 1**

Activation energy [kJ/mol]	Peak 1	Peak 2	Peak 3
No aging	-	31.4	43.9
48 h aging	39	46.3	62.8

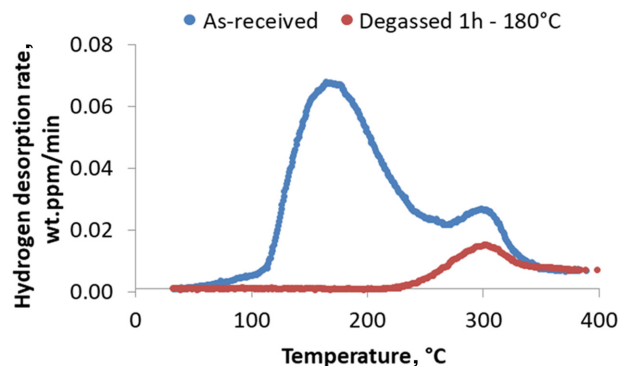


**Fig. 6. Effect of degassing on hydrogen desorption spectrum for non-aged samples from steel grade 1**

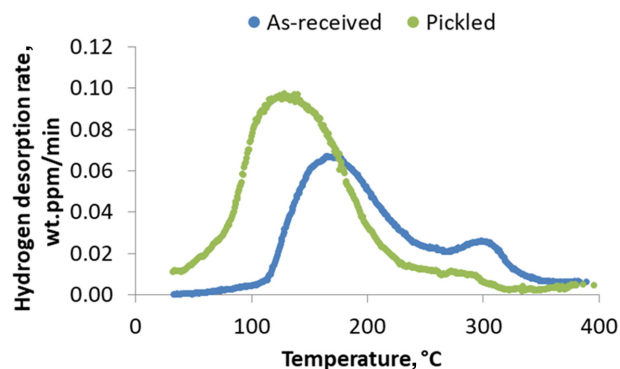


**Fig. 7. Effect of pickling on hydrogen desorption spectrum for non-aged samples from steel grade 1**

pickling respectively, for samples collected from the steel part that was not aged for steel grade 1. They enable to

observe the effect of the zinc coating on thermal desorption analysis and on hydrogen degassing capability of the material. As a complement, diffusible hydrogen content obtained in steel grade 1 after degassing (red curve of Fig. 6) is  $0.18 \pm 0.04$  wt.ppm, while equivalent samples after pickling exhibit  $0.74 \pm 0.05$  wt.ppm of diffusible hydrogen.

## 4. Discussion

### 4.1 Initial level of diffusible hydrogen content in steel grades

First of all, the definition of the reference level of diffusible hydrogen content in both grades is essential. Indeed, it is important for this study to show that hydrogen distribution along the steel sheet is homogeneous. Quite limited error bars obtained for reference levels measured in the metal bulk (Table 1) and the fact that reference levels are in good coherence with diffusible hydrogen contents localized farther from the cut edge (at distances around 6 to 9 mm for steel grade 1 and at longer distances of 30 mm for steel grade 2, observed in Fig. 3) enable to support the hypothesis of a quite uniform distribution of hydrogen around the sheets.

It can also be observed from Table 1 that the two studied DP780GI exhibit quite different initial levels of diffusible hydrogen content. This can be impacted by different factors. Firstly, specific annealing conditions have been considered on one of the two DP780GI to maximize the initial hydrogen content and compare hydrogen behavior within two materials exhibiting very different initial diffusible contents. Indeed, annealing temperature, duration

and atmosphere have a strong impact on resulting hydrogen uptake. Furthermore, the storage way can also have an influence on initial hydrogen content of industrial coils. Indeed, hydrogen uptake in such steels occurs generally during high temperature operations, when bare steel is furthermore exposed to atmospheric sources of hydrogen. Afterwards, zinc coating is known to have a barrier effect to hydrogen diffusion at room temperature [7-9]. In this regard, hydrogen degassing mainly occurs through bare edges in a galvanized steel sheet. Both steel grades were chosen for this study because it is interesting to compare hydrogen behavior within two materials exhibiting very different initial diffusible contents.

#### 4.2 Effect of aging on hydrogen spatial distribution in steel grades

The effect of the aging clearly appears for both steel grades in Fig. 3. As observed, a hydrogen segregation is observed in the near cut edge range: for steel grade 1, the diffusible hydrogen amount is twice the reference level, while on steel grade 2 it is even thrice. For the 1<sup>st</sup> steel grade, this H segregation near the cut edge seems to be accompanied by a slight H depletion in its neighborhood, before reaching again the reference level within a few millimeters of distance from the cut edge. For steel grade 2, this depletion is not observed and the H segregation starting from the cut edge extends on longer distances than for steel grade 1.

At first view, hydrogen segregation in the cut edge is quite surprising. Indeed, bare edges are known to constitute preferential paths for hydrogen desorption in galvanized steels. In DP steels, microstructure is constituted of ferrite and martensite. When shear cutting is applied, the steel microstructure is damaged around the cut zone [10]. Indeed, shear cutting introduces a strain-hardened zone of about 100  $\mu\text{m}$ -width next to the cut edge, which is full of dislocations. As dislocations constitute a trap for hydrogen atoms, this phenomenon could explain the segregation of hydrogen in this zone.

Regarding the distance on which this H segregation is observed in both steels, the significantly larger distance observed for steel grade 2 could be related to its initial lower value in terms of diffusible hydrogen. Segregation at the cut edge surface could in this case deplete more rapidly its neighborhood and exacerbate the H gradient concentration

between edge and bulk, which constitute the driving force for hydrogen diffusion [11] from bulk to edges.

#### 4.3 Effect of aging on hydrogen desorption spectra

Hydrogen segregation near the cut edge also impacts hydrogen desorption spectra, as highlighted in Fig. 4. Indeed, the segregation of hydrogen in the 48h aging sample is accompanied by the appearance of a third contribution in the hydrogen desorption peak. For the sake of clarity, let's define the different contributions to the hydrogen desorption spectrum as follows: peak 1 is defined as the contribution whose maximal desorption rate is observed at around 80 °C, peak 2 at 180 °C and peak 3 at 300 °C (Fig. 4).

As peak 1 exists only for the samples collected in the H-segregated zone near the cut edge, it clearly appears that it should be related to this segregation. It thus seems that this 1<sup>st</sup> peak is associated with hydrogen that was able to migrate towards the cut edge during the 48 h aging, and which is likely located in dislocations traps near the bare edge. A slight thermal energy provided by the initiation of the heating in TDA is sufficient to let this amount desorb very rapidly, due to its proximity with the bare edge.

For the non-aged samples, this peak 1 contribution does not appear, even partially at a lower scale. However, edges are also bare and should promote hydrogen degassing through them. Furthermore, as a reminder, the small dimensions of the analyzed samples (3 × 10 × 2 mm-thick) ensure a quite close proportion between bare and coated surfaces of this type of sample. The absence of peak 1 contribution for non-aged samples could be explained by the fact that dislocations in the near cut edge range seem also to play the role of hydrogen traps, which in the first instance of TDA heating are first filled, before letting finally hydrogen degas.

Peaks 2 and 3 are observed on their side for all the other samples and thus seem to be fully representative of the overall system, which is constituted of the DP steel substrate and the GI coating. The appearance of a diffusible hydrogen peak at around 180 °C (peak 2) for the used heating rate is quite common for ferritic steels [12,13]. However, the presence of a second contribution (peak 3) at 300 °C is more scarce. Different hypotheses can be evoked.

Firstly, the existence of both contributions could be related to the co-existence of two phases in the DP steel grade: ferrite and martensite. Each phase involves different hydrogen diffusion coefficients and traps. More specifically, martensite is a strongly deformed body-centered cubic phase which contains lots of dislocations. Martensite thus exhibits a deformed crystalline structure, compared to ferrite, while it also contains a high density of traps. Both parameters tend to slow hydrogen diffusion in martensite with respect to ferrite. Secondly, the relative proportion of martensite and ferrite is also important, as well as their percolation level [14,15]. The presence of the zinc coating could on its side also affect hydrogen desorption phenomena. Indeed, it is already well known that Zn can play the role of hydrogen barrier at room temperature. Furthermore, it could induce trapping sites, either intrinsically or through its interface with the steel substrate. This interface is constituted of the zinc coating, of the intermetallic layer and of the steel substrate [7-9,16]. All those features can constitute potential traps for hydrogen or barriers to hydrogen diffusion.

In order to investigate those different hypotheses, specific experiments were performed, as illustrated in Figs 5, 6 and 7 and as inspired by the methodology developed in [17]. In order to assess the hypothesis of different traps for hydrogen in the global system (steel or coating), Kissinger's methodology was applied for steel grade 1 and the effect of preliminary aging on peak evolution with desorption rate was analyzed (Fig. 5). This led to the obtention of activation energies reported in Table 2. De-trapping energies are commonly considered as corresponding to reversible hydrogen traps when they do not exceed a limit defined as 50 kJ/mol and irreversible if they do [18]. The computation of activation energies gives rise to quite surprising results. Firstly, peak 2, which exhibits a common desorption temperature for aged and non-aged samples, would according to this result correspond to quite different activation energies for both steels. In non-aged samples, it could correspond to dislocations [19-20], which is typically expected in that type of microstructure, while it is not the case after room temperature aging (nearly considered as irreversible). Furthermore, activation energies associated to peak 3 would also correspond to (nearly) irreversible hydrogen traps.

Degassing experiments were led in order to assess the reversible nature of hydrogen traps associated with peak contributions 2 and 3. Degassing experiments could have been operated at room temperature, but 180 °C was chosen in order to accelerate potential degassing. Fig. 6 shows that degassing during 1h is sufficient to fully desorb hydrogen contribution to peak 2 and partially desorb peak 3, tending to confirm their reversible trap nature. This thus tends to discredit the first hypothesis of an irreversible trap nature suggested by activation energy results.

Finally, pickling experiments were performed in order to remove the GI coating in order to qualify the effect of this coating on H desorption spectra. In terms of diffusible content, we see that pickling leads to a slight hydrogen uptake (around 0.10 wt.ppm in the studied conditions). This is due to the fact that pickling implies reaction of Zn with HCl, forming dihydrogen as byproduct. Part of it can be absorbed by the material [16]. Even if this artifact impedes the verification of the conservation of diffusible hydrogen content before and after pickling, we can assume few losses of hydrogen during pickling. In terms of impact of pickling on hydrogen desorption spectra (Fig. 7), the removal of the coating leads to one major contribution at a temperature slightly lower than peak 2 temperature, with a slight shoulder of the peak towards higher temperatures. The slight shift towards lower temperature of peak 2 seems to confirm that the Zn coating is playing the role of a slight diffusion barrier, compared to bare surface. The slight shoulder observed at larger temperatures is more difficult to interpret. Indeed, it could be due to a deeper trapping in the material, as initially suggested by the related activation energies, or to hydrogen trapped at the zinc / steel interface.

By comparing different experiments, those discrepancies between aged and non-aged samples question the scientific soundness of applying Kissinger's methodology in this particular framework. Indeed, the latter method is based on the fact that de-trapping should govern the desorption mechanism. If diffusion tended to govern the desorption process, for instance through a diffusion-limiting phase or coating, activation energy would contain contributions of diffusion and de-trapping, which can thus not be straightforwardly compared to literature data compiling H trap energies [21,22]. Hydrogen thus seems to be mainly present in reversible traps in the steel substrate or at the steel-

coating interface and its diffusion paths towards outside seem to be responsible for particular desorption curve shape.

## 5. Conclusions

In this study, the objective was to investigate why a time delay between punching and expanding holes (following ISO16630 standard) induces a detrimental effect on the edge cracking limit. A main hypothesis was related to the presence of diffusible hydrogen in those materials: during the time between punching and expanding holes, a hydrogen migration towards the punched edges was suggested and could lead to preferential hydrogen embrittlement.

As a result, the use of a newly-developed TDA set-up dedicated to small samples ensured to quantify diffusible hydrogen near cut edges. Based on induction heating, this set-up indeed offers very flexible heat cycles. Furthermore, Zn-coated samples can be analyzed without zinc removal, as the sample dimensions permit hydrogen desorption through bare edges. The latter enables to limit the artifacts that can be associated to hydrogen measurement.

Owing to this method, a hydrogen gradient was highlighted on short-range distances for shear-cut galvanized steel sheets after a certain time. Hydrogen migration towards cut-edges was evidenced and was explained by a potential trapping in dislocations of the work-hardened zone induced by shear cutting. This was shown to have a direct influence on hydrogen desorption spectra, constituted of 2 or 3 main contributions for non-aged and aged samples respectively.

Hydrogen diffusion and desorption paths were discussed. During TDA, for non-aged samples, hydrogen first accumulates in dislocation traps near cut edges, before massively desorbing through bare and coated surfaces. For aged samples, hydrogen preliminarily absorbed in dislocations desorbs more rapidly through bare edges, owing to their segregation in the proximity of the bare edge, constituting a rapid diffusion path. The massive desorption occurring through 2<sup>nd</sup> peak is shown to be affected by Zn coating: acting as a hydrogen diffusion barrier, it slows down diffusion and shifts the peak towards slightly larger temperatures. Finally, the 3<sup>rd</sup> peak is more complicated to interpret and could be due to a deeper trap (in the steel substrate or at zinc/steel interface).

## References

1. N. Fonstein, *Advanced High Strength Steels – Physical Metallurgy, Design, Processing, and Properties*, Springer (2015).
2. ISO16630:2017, *Metallic materials – Sheet and strip – Hole expanding test*, International Organization for Standardization, Geneva (2017). <https://cdn.standards.iteh.ai/samples/69771/f270c79a7a3a4975a676505fcb65f5d/ISO-16630-2017.pdf>
3. N. Winzer, T. Schaffner, V. Kokotin, and R. Thiessen, *Proc. 4th international conference on metals & hydrogen (SteelyHydrogen 2022)*, Ghent, Belgium (2022).
4. E. Atzema, and P. Seda, *Proc. SCT Steels in Cars and Trucks*, Amsterdam-Schiphol, Netherlands (2017).
5. H. E. Kissinger, *Reaction Kinetics in Differential Thermal Analysis*, *Analytical Chemistry*, **29**, 1702 (1957). Doi: <http://dx.doi.org/10.1021/ac60131a045>
6. K. Bergers, E. Camisão de Souza, I. Thomas, N. Mabho, and J. Flock, *Determination of hydrogen in Steel by Thermal Desorption Mass Spectroscopy*, *Steel Research International*, **81**, 499 (2010). Doi: <https://doi.org/10.1002/srin.201000023>
7. M. Mandy, B. Nabi, M. Larnicol, X. V. Eynde, C. Georges and F. E. Goodwin, *Influence of Zn-based Coating Alloys on Hydrogen Diffusion and Corrosion Resistance in a DP Steel*, *BHM Berg- und Hüttenmännische Monatshefte*, **166**, 554 (2021). Doi: <https://doi.org/10.1007/s00501-021-01160-9>
8. K. R. Jo, L. Cho, D. H. Sulistiyo, E. J. Seo, S. W. Kim, and B. C. De Cooman, *Effect of Al-Si coating and Zn coating on the hydrogen uptake and embrittlement of ultra-high strength press-hardened steel*, *Surface and Coatings Technology*, **374**, 1108 (2019). Doi: <https://doi.org/10.1016/j.surfcoat.2019.06.047>
9. D. H. Coleman, B. N. Popov, R. E. White, *Hydrogen permeation inhibition by thin layer Zn-Ni alloy electrodeposition*, *Journal of Applied Electrochemistry*, **28**, 889 (1998). Doi: <https://doi.org/10.1023/A:1003408230951>
10. A. Lara, I. Picas, and D. Casellas, *Effect of the cutting process on the fatigue behaviour of press hardened and high strength dual phase steels*, *Journal of Materials Processing Technology*, **213**, 1908 (2013). Doi: <https://doi.org/10.1016/j.jmatprotec.2013.05.003>
11. Y. Fukai, *The Metal-Hydrogen System – Basic Bulk Properties*, Springer (2005).
12. C. Georges, T. Sturel, P. Drillet, and J.-M. Maitaigne, *Absorption/Desorption of Diffusible Hydrogen in Alumi-*

- nized Boron Steel, *ISIJ International*, **53**, 1295 (2013). Doi: <https://doi.org/10.2355/isijinternational.53.1295>
13. L. Cho, D. H. Sulistiyo, E. J. Seo, K. R. Jo, S. W. Kim, J. K. Oh, Y. R. Cho, and B. C. De Cooman, Hydrogen absorption and embrittlement of ultra-high strength aluminumized press hardening steel, *Materials Science and Engineering: A*, **734**, 416 (2018). Doi: <https://doi.org/10.1016/j.msea.2018.08.003>
  14. Z. Wang, J. Liu, F. Huang, Y.-J. Bi, and S.-Q. Zhang, Hydrogen Diffusion and Its Effect on Hydrogen Embrittlement in DP Steels With Different Martensite Content, *Frontiers in Materials*, **7**, 1 (2020). Doi: <https://doi.org/10.3389/fmats.2020.620000>
  15. S. Frappart, A. Oudriss, X. Feaugas, J. Creus, J. Bouhattate, F. Thébault, L. Delattre, and H. Marchebois, Hydrogen trapping in martensitic steel investigated using electrochemical permeation and thermal desorption spectroscopy, *Scripta Materialia*, **65**, 859 (2011). Doi: <https://doi.org/10.1016/j.scriptamat.2011.07.042>
  16. P. Maass, and P. Peissker, C. Ahner, Handbook of Hot-dip Galvanization, Wiley-Vch (2011).
  17. M. Krid, M. Mandy, T. Sturel, R. Grigorieva, P. Drillet, and P. J. Jacques, A better understanding of hydrogen trapping and diffusion in aluminumized press-hardenable steels, *Journal of Materials Research and Technology*, **28**, 1514 (2023). Doi: <https://doi.org/10.1016/j.jmrt.2023.11.214>
  18. T. Michler, and M. P. Balog, Hydrogen environment embrittlement of an ODS RAF steel-Role of irreversible hydrogen trap sites, *International Journal of Hydrogen Energy*, **35**, 9746 (2010). Doi: <https://doi.org/10.1016/j.ijhydene.2010.06.071>
  19. J. Venezuela, Q. Liu, M. Zhang, Q. Zhou, and A. Atrens, A review of hydrogen embrittlement of martensitic advanced high-strength steels, *Corrosion Reviews*, **34**, 153 (2016). Doi: <https://doi.org/10.1515/correv-2016-0006>
  20. F. G. Wei, and K. Tsuzaki, Hydrogen trapping phenomena in martensitic steels, In: Gaseous hydrogen embrittlement of materials in energy technologies (Vol. 1), pp. 493 - 525, Woodhead Publishing Limited (2012). Doi: <https://doi.org/10.1533/9780857093899.3.493>
  21. H. K. D. H. Badeshia, Prevention of Hydrogen Embrittlement in Steels, *ISIJ International*, **56**, 24 (2016). Doi: <https://doi.org/10.2355/isijinternational.ISIJINT-2015-430>
  22. K. Verbeken, Analysing hydrogen in metals: bulk thermal desorption spectroscopy (TDS) methods In: Gaseous hydrogen embrittlement of materials in energy technologies (Vol. 1), pp. 27 - 55, Woodhead Publishing Limited (2012). Doi: <https://doi.org/10.1533/9780857095374.1.27>